Sino Biological
Tag Antibody As Low As
$59
Only $38/ each for
Hot Cytokines & Growth Factors
50% off
for All ELISA Kits and Pair Sets

The Journal of Immunology

The Extracellular Membrane-Proximal Domain of Human Membrane IgE Controls Apoptotic Signaling of the B Cell Receptor in the Mature B Cell Line A20

Monica Poggianella, Marco Bestagno and Oscar R. Burrone

J Immunol 2006; 177:3597-3605; ;
doi: 10.4049/jimmunol.177.6.3597
http://www.jimmunol.org/content/177/6/3597

This information is current as of September 26, 2017.

References This article **cites 47 articles**, 26 of which you can access for free at:
http://www.jimmunol.org/content/177/6/3597.full#ref-list-1

Subscription Information about subscribing to *The Journal of Immunology* is online at:
http://jimmunol.org/subscription

Permissions Submit copyright permission requests at:
http://www.aai.org/About/Publications/JI/copyright.html

Email Alerts Receive free email-alerts when new articles cite this article. Sign up at:
http://jimmunol.org/alerts

The Journal of Immunology is published twice each month by
The American Association of Immunologists, Inc.,
1451 Rockville Pike, Suite 650, Rockville, MD 20852
Copyright © 2006 by The American Association of Immunologists All rights reserved.
Print ISSN: 0022-1767 Online ISSN: 1550-6606.

Downloaded from http://www.jimmunol.org/ by guest on September 26, 2017

The Extracellular Membrane-Proximal Domain of Human Membrane IgE Controls Apoptotic Signaling of the B Cell Receptor in the Mature B Cell Line A20

Monica Poggianella, Marco Bestagno, and Oscar R. Burrone[1]

Ag engagement of BCR in mature B cells can deliver specific signals, which decide cell survival or cell death. Circulating membrane IgE$^+$ (mIgE$^+$) cells are found in extremely low numbers. We hypothesized that engagement of an εBCR in a mature isotype-switched B cell could induce apoptosis. We studied the role of the extracellular membrane-proximal domain (EMPD) of human mIgE upon BCR engagement with anti-Id Abs. Using mutants lacking the EMPD, we show that this domain is involved in controlling Ca^{2+} mobilization in immunoreceptors of both γ and ε isotypes, as well as apoptosis in signaling originated only from the εBCR. We mapped to the εCH4 ectodomain the region responsible for apoptosis in EMPD-deleted receptors. Ca^{2+} mobilization was not related to apoptotic signaling. This apoptotic pathway was caspase independent, involved ERK1/2 phosphorylation and was partially rescued by CD40 costimulation. We therefore conclude that the EMPD of human mIgE is a key control element of apoptotic signaling delivered through engagement of εBCR within the context of a mature B cell. ***The Journal of Immunology,*** **2006, 177: 3597–3605.**

Membrane Igs (mIgs)[2] (1) expressed on the surface of B lymphocytes differ from their secretory counterparts for the presence of three additional domains at the C terminus of the H chain, namely: the extracellular membrane-proximal domain (EMPD), the transmembrane domain (TMD), and the cytoplasmic domain (CytoD). The TMD, in addition to supporting the insertion of Igs in the cell membrane, participates in the assembly of the BCR with the accessory molecules of the complex CD79a (Igα) and CD79b (Igβ) (1–3). The cytoplasmic portions of mIgs show high variability in sequence and length, although isotypes α, ε, and γ present a conserved tyrosine-containing motif, which has been involved in Ag internalization and degradation (4–8). In contrast, the structure and function of the EMPD of cell-bound Igs are largely unknown. The EMPDs of different Ig isotypes have different lengths and a low degree of sequence homology, although sharing a large number of acidic residues (9). The extracellular location tethering the Ig Fc region to the cell membrane, as well as the differences in sequence and lengths, most likely determine a role in BCR assembly and may be associated with isotype-specific functions. In most cases, with the exception of the μ and the δ isotypes, cysteine residues located within the EMPD contribute to the stabilization of the membrane protein through the formation of interchain disulfide bridges (9). In the case of human IgE, two membrane isoforms differing in the length of the EMPD (ε-long isoform (ε_L) and ε-short isoform (ε_{Sh})) are generated as a consequence of alternative splicing in the penultimate exon (M1) of the membrane ε H chain transcript. The longer variant uses an acceptor splice site that is located 156 nt upstream of the acceptor site used to generate the short one. As a consequence, the two membrane isoforms have the same ε C region and the same TMD and CytoD, but differ in a 52-aa segment within the EMPD. The ε_{Sh} EMPD contains 14 aa, while the ε_L is extended at the N terminus encoding a total of 66 aa (9–11). Both membrane isoforms were shown to form functional BCRs capable of transducing cellular responses upon cross-linking (12). Differences in the level of glycosylation of the Igα (CD79a) molecules, depending on the EMPDs of the associated human mIgE (short or long) as well as of human IgM and IgD, have been previously described (12, 13). In addition, the EMPD has been implicated in the different apoptotic signaling observed for IgM and IgD (14) and, in particular for IgE, the short EMPD isoform was apoptotic in the immature B cell line WEHI-231, while the long was not (12). It is generally assumed that in immature (mIgM$^+$) and mature (mIgM$^+$/mIgD$^+$) B lymphocytes Ag contact leads to cell differentiation, cell death or anergy, while in mature isotype-switched B cells (mIgG$^+$, mIgE$^+$ or mIgA$^+$) and memory B cells it leads to cell proliferation. Within germinal centers, a selection of high affinity Ag-specific B cell repertoire against low-affinity cells and Ig isotype switch (from IgM to IgA, IgG, or IgE) takes place. B cell fate in these lymph nodes is under the control of CD40 survival signaling and Fas death signaling (15).

Serum IgE levels are much lower than those of all other Ig isotypes and, in agreement with the requirement of membrane expression for the production of the secretory serum form (6), circulating mIgE$^+$ B cells are rare and difficult to visualize. We therefore investigated whether IgE expression in the context of the mature isotype-switched B cell line A20 could deliver apoptotic signaling similar to the effect produced by anti-IgE mAbs (16).

In this study, we show that the EMPD and εCH4 ectodomains of mIgE play essential roles in determining the outcome of cell signaling, following BCR engagement.

International Centre for Genetic Engineering and Biotechnology, Trieste, Italy

Received for publication August 5, 2005. Accepted for publication June 26, 2006.

The costs of publication of this article were defrayed in part by the payment of page charges. This article must therefore be hereby marked *advertisement* in accordance with 18 U.S.C. Section 1734 solely to indicate this fact.

[1] Address correspondence and reprint requests to Dr. Oscar R. Burrone, International Centre for Genetic Engineering and Biotechnology, Padriciano 99, 34012 Trieste, Italy. E-mail address: burrone@icgeb.org

[2] Abbreviations used in this paper: mIg, membrane Ig; $\Delta\psi m$, transmembrane potential; CytoD, cytoplasmic domain; ε_L, ε-long isoform; EMPD, extracellular membrane-proximal domain; ε_{Sh}, ε-short isoform; mSIP, membrane small immunoprotein; PARP, poly(ADP-ribose) polymerase; PI, propidium iodide; SIP, small immune protein; TMD, transmembrane domain; wt, wild type; z-VAD-fmk, *N*-benxyloxycarbonyl-Val-Ala-Asp(Ome)-fluoromethylketone.

Copyright © 2006 by The American Association of Immunologists, Inc.

0022-1767/06/$02.00

Downloaded from http://www.jimmunol.org/ by guest on September 26, 2017

Materials and Methods

DNA constructs

The plasmids for the expression of the two complete membrane ε H chain isoforms have already been described (11). The ε-ΔEMPD was obtained from the previously described pCDNA-ε-membrane small immunoprotein (mSIP)/ΔEMPD (9) by transferring a *Bsu36I*/*Xba*I fragment (from εCH4 to the stop codon) into the full-length ε construct. All other gene constructs were cloned into the pCDNA3 plasmid (Invitrogen Life Technologies). The constructs encoding γ1-mSIP and ε-mSIPs with EMPD long, EMPD short, without EMPD, or with human γ1 EMPD have been described previously (9). Plasmids encoding ε_L-mSIP/ΔCyto and ε_{Sh}-mSIP/ΔCyto were obtained respectively by PCR amplification of the regions coding for εCH4-EMPD-TMD with primers 5′-CTGAGGACACGGCCGTCTAT TACTG-3′ and 5′-GTTAGGATCCTCGCTGCACCATGAGGAGCGT-3′. The resulting fragments were digested with Bsu36I and *Bam*HI and ligated to the corresponding ε_L-mSIP and ε_{Sh}-mSIP plasmids. ε-mSIP/ΔEMPD/ΔCyto was obtained by transferring a *Kas*I/*Kas*I fragment from ε_L-mSIP/ΔCyto (which contained the TMD, followed by a stop codon and the poly(A) site) into ε-mSIP/ΔEMPD. The ε-mSIP/ΔEMPD-GPI was obtained by substitution of the fragment coding for TMD and CytoD from ε-mSIP/ΔEMPD vector with a GPI signal sequence (17). Construct γ1-mSIP/ΔEMPD was generated by PCR amplification of the γ1 TMD and CytoD with primers 5′-CTTGGATCCGGGCTGTGGACGACCATCA CC-3′ and 5′-CTGAATTCTTAGGCCCCCTCTCCGATCATGT-3′. The PCR fragment was inserted into the *Bam*HI/*Eco*RI sites of ε-mSIP/ΔEMPD to produce the chimera ε-mSIP/ΔEMPD/γ1-TMD-CytoD. In this plasmid, the *Bsp*EI-*Bam*HI εCH4 domain was finally substituted by γ1CH3 domain obtained by PCR amplification with sense primer (5′-TA CTCCGGAGGCTCTGGCGGGCAGCCCCGAGAACCACA-3′) and antisense primer (5′-GATGGATCCCGGGGACAGGGAGAGGCTCTTG-3′).

To generate the chimera γ1-mSIP/ΔEMPD/ε-TMD-CytoD, the εCH4 domain was substituted by γ1CH3 domain, obtained as described above, in ε-mSIP/ΔEMPD. The ΔεCH4 constructs were obtained by deleting the fragment from *Bsp*EI at the 5′ to the *Xma*I site at the 3′ end of εCH4 domain. To obtain anti-idiotypic Abs (by DNA immunization), the Id in the single-chain variable fragment format (in all cases as *Hind*III-*Bsp*EI fragments, with V_L-linker-V_H orientation) were cloned into vectors encoding secretory γ1-SIP (18) or ε-SIP (19).

Mice and guinea pig immunization and sera analysis

BALB/c mice were vaccinated three times at 2-wk intervals with 1 μg of plasmid by gene-gun technique (20, 21). Fifteen days after the last boost, blood was collected via retro-orbital puncture. For guinea pig immunizations, 2 μg of DNA per shot was used, and sera were collected by cardiac puncture. Immune responses against the Id were analyzed by cytofluorimetry on a FACSCalibur (BD Biosciences) using anti-Id sera, followed by FITC-conjugated goat anti-mouse IgG or anti-guinea pig IgG Abs (Kirkegaard & Perry Laboratories).

IgG purification and IgG Fab production

Sera, obtained from vaccinated guinea pigs, were purified using DEAE Affi-Gel BLUE GEL (Bio-Rad), following the manufacturer's protocol. IgG fractions were quantified by SDS-PAGE, followed by Coomassie staining, and by spectrophotometry. A total of 200 μg of purified IgG, resuspended in PBS, was digested at 37°C for 3 h with 0.02 mg/ml papain (twice crystallized; Sigma-Aldrich) in PBS containing 10 mM EDTA and 5 mM cysteine. The reaction was stopped by addition of iodoacetamide (final concentration 30 mM) and dialyzed at 4°C against PBS. Digestion products were analyzed in 10% nonreducing SDS-PAGE, stained with Coomassie blue.

Cell lines and transfections

The murine myeloma B cell line Sp2/0, the mouse B lymphoma A20 (American Type Culture Collection; TIB-208), and the FcγR-negative variant A20IIA1.6 (22) (provided by C. Bonnerot, Institut Curie, Paris, France) were maintained in RPMI 1640 with Glutamax I (Invitrogen Life Technologies) and 25 mM HEPES, supplemented with 10% heat-inactivated FCS, 50 μg/ml gentamicin, 1 mM sodium pyruvate, and 0.5 μM 2-ME. Transfections were performed by electroporation, as described previously (9). The Sp2/0, A20, and A20IIA1.6 stable clones were cultured in selective medium containing 400 μg/ml G-418 (Geneticin; Invitrogen Life Technologies).

BCR cross-linking and capping

For cross-linking experiments, cells (5×10^4 in 100 μl of complete medium) were treated with the different Abs: goat anti-human IgE (20 μg/ml; Kirkegaard & Perry Laboratories); goat anti-human IgG (20 μg/ml; Kirkegaard & Perry Laboratories); goat anti-mouse IgG (20 μg/ml; Kirkegaard & Perry Laboratories); mouse (5–10 μl) or guinea pig (1–5 μl) anti-Id sera; guinea pig IgG purified from anti-Id sera (20 μg); and the corresponding IgG Fab (20 μg). Monoclonal hamster anti-mouse Fas (clone Jo2; BD Pharmingen) was used at 1 μg/ml, or rat anti-mouse CD40 (Southern Biotechnology Associates) at 10 μg/ml and monoclonal rat anti-mouse CD16/CD32 (clone 2.4G2; BD Pharmingen) at 50 μg/ml. The anti-Id sera used to cross-link ε-mSIPs and mIgE were derived from animals vaccinated with plasmids coding for secretory γ1-SIP, while the ones for γ1-mSIPs were obtained from animals immunized with vectors coding for secretory ε-SIP, as described above.

Assay of the effect of secretory ε-SIP on A20 wild-type (wt) cells was performed using 100 μl of supernatant from Sp2/0 cell transfectant and 1 μl of anti-Id serum on 5×10^4 A20 cells.

For capping experiments, 2×10^5 cells were resuspended in 400 μl of medium and cross-linked for 15 min at 37°C or 4°C with goat anti-mouse IgG FITC conjugated (Kirkegaard & Perry Laboratories) or anti-Id. In the latter case, after washing, cells were incubated for 40 min at 4°C with FITC-labeled goat anti-human IgE or anti-human IgG. Cells were then allowed to adhere to poly(lysine) (Sigma-Aldrich)-coated coverslips, fixed with 4% paraformaldehyde for 5 min, mounted with Prolong Gold (Molecular Probes), and analyzed by fluorescence microscopy (Leica Microsystems).

Apoptosis analysis

Apoptosis was determined by flow cytometry with the annexin V-FITC/PI assay. In brief, cells were collected, washed in PBS, resuspended in 200 μl of annexin buffer (10 mM HEPES/NaOH (pH 7.4), 140 mM NaCl, 5 mM $CaCl_2$) containing Annexin V^{FITC} (Roche), diluted 1/400, and 1 μg/ml propidium iodide (PI; Molecular Probes), and incubated for 30 min at room temperature in the dark. For testing caspase and cathepsin inhibition, cells in complete medium were preincubated for 2 h with the broad caspase inhibitor *N*-benxyloxycarbonyl-Val-Ala-Asp(Ome)-fluoromethylketone (Z-VAD-fmk; 25 μM; Sigma-Aldrich) or with the cathepsin inhibitor Loxistatin (100 μM) (Sigma-Aldrich) before the cross-linker addition. The inhibition effect on cell death was investigated by annexin-PI assay, as described above.

DNA analysis

To analyze cellular DNA content, cells were incubated for 30 min in the dark at room temperature in hypotonic solution (0.1% sodium citrate, 0.1% Nonidet P-40 (Calbiochem), and 50 μg/ml RNase) containing 50 μg/ml PI (Molecular Probes). PI fluorescence was determined by cytofluorimetry. DNA fragmentation was analyzed from 10^6 cells cross-linked with anti-Id or anti-mouse Fas. Cells were lysed in TNE buffer (100 mM Tris-HCl (pH 8.0), 200 mM NaCl, 5 mM EDTA) containing 0.2% SDS and 200 μg/ml proteinase K and incubated overnight at 37°C. DNA was extracted by phenol-chloroform and ethanol precipitated. Samples were dissolved in TE (10 mM Tris-HCl (pH 8.0), 1 mM EDTA) buffer, treated for 2 h with 50 μg/ml RNase A at 37°C, and analyzed by electrophoresis on 1.8% agarose gel. Chromatin condensation analysis was performed in cells fixed with paraformaldehyde for 10 min at room temperature, stained with Hoechst 33258 (1 mg/ml in PBS) for 20 min at 37°C, and examined by fluorescence microscopy.

Mitochondrial transmembrane potential (Δψm)

Changes in the mitochondrial Δψm were determined by staining cells for 30 min at 37°C with 25 nM Mitotracker orange reagent (CMTMRos; Molecular Probes). After PBS washing, cells were analyzed by cytofluorimetry.

Poly(ADP-ribose) polymerase (PARP) cleavage analysis

After 6-h cross-linking, 5×10^5 cells were lysed for 10 min on ice in TNN buffer (250 mM NaCl, 50 mM Tris-HCl (pH 8), 0.5% Nonidet P-40) containing PMSF and protease inhibitor mixture (Sigma-Aldrich), and centrifuged at 16,000 × *g* for 15 min at 4°C. Supernatants were run on 8% SDS-PAGE and transferred to polyvinylidene difluoride membranes (Millipore) for Western blotting. Membranes were saturated in PBS with 0.1% Tween 20 (Sigma-Aldrich) and 5% nonfat dry milk, and incubated with 1 μg/ml monoclonal mouse anti PARP (clone C2-10; BD Pharmingen). After

Downloaded from http://www.jimmunol.org/ by guest on September 26, 2017

subsequent incubation with HRP-conjugated goat anti-mouse IgG (Kirkegaard & Perry Laboratories), proteins were revealed using ECL (Amersham Biosciences).

ERK1/2 MAPK activation

Analysis of ERK activation was conducted in lysates of cross-linked cells (5×10^5) run in 10% SDS-PAGE, transferred to polyvinylidene difluoride membrane, and incubated overnight at 4°C with monoclonal anti-phospho-p44/42 MAPK (clone E10) or anti-p42 MAPK (clone 3A7), both from Cell Signaling Technology, at 1/2000 dilution in 5% nonfat dry milk in TBST, followed by incubation with goat anti-mouse IgG-HRP Ab (Kirkegaard & Perry Laboratories). Protein bands were detected by ECL.

Ca^{2+} mobilization assay

Cells (10^7) were washed and resuspended in 0.5 ml of complete medium containing 10 μM Fluo-3AM (Molecular Probes), incubated for 30 min at 37°C, and after addition of 10 ml of HBSS buffer (118 mM NaCl, 4.6 mM KCl, 10 mM glucose, 20 mM HEPES (pH 7.2)) were further incubated for additional 30 min at 37°C. Cells were then washed with 10 ml of HBSS and finally resuspended in 10 ml of complete medium. Usually, 3×10^5 Fluo-3AM-charged cells were used for Ca^{2+} level measurements by flow cytometry after stimulation with goat anti-mouse IgG (20 μg/ml) or anti-Id.

Results

ε Immunoreceptors and Ca^{2+} mobilization

In this study, we used full-length mIgE and reduced-size membrane-bound immunoreceptors (called mSIP) to obtain stable transfectant clones of the murine mature IgG^+ B cell line A20. mSIPs consist of a single-chain variable fragment Ab (V_L-linker-V_H) fused to the C-terminal region of a mIg H chain, from the last dimerizing domain of Fc, CH4 (for μ and ε) or CH3 (for γ, δ, and α), down to the cytoplasmic tail (Fig. 1). These molecules are efficiently folded and expressed as dimers on the surface of transfected cells and, in the case of ε, γ, and α, they are covalently stabilized through disulfide bonds between cysteines present in the EMPD (9, 20, 21). In addition, normal signaling of A20 expressing mSIPs of ε and γ1 isotypes (ε_L-mSIP, ε_{Sh}-mSIP, and γ1-mSIP) was confirmed by analyzing their ability to promote intracellular Ca^{2+} mobilization upon cross-linking. As shown in Fig. 2*A*, full-length IgE, as well as the ε- and γ1-mSIPs, induced a Ca^{2+} signal comparable to that of the endogenous murine IgG expressed by A20 cells, indicating efficient triggering of this early event of the BCR signaling cascade. In agreement with these data, capping of these receptors after cross-linking was also observed, further confirming normal anchoring to the cell membrane (Fig. 2*B*).

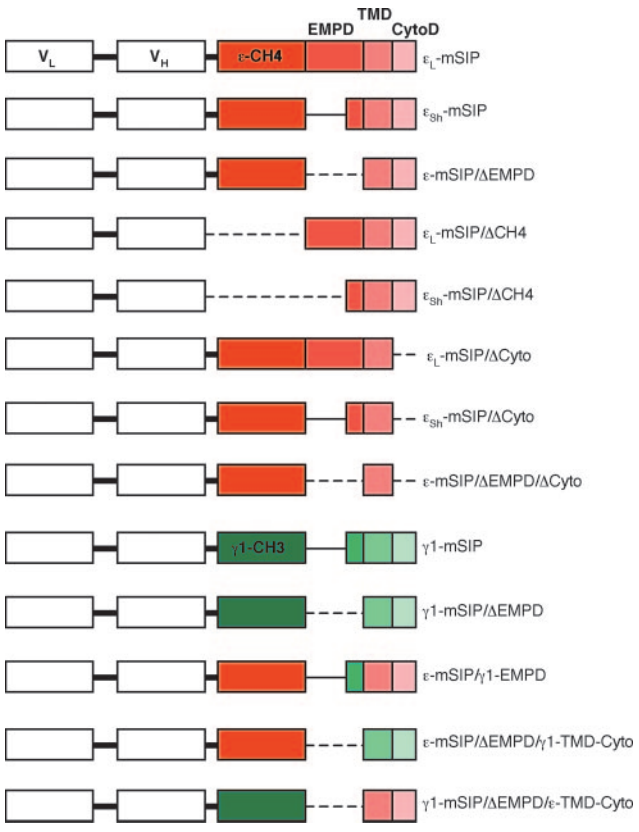

FIGURE 1. Schematic representation of the different membrane constructs used to transfect murine B cell line A20. Boxes correspond to defined domains, thick lines to linker sequences, while thin lines indicate naturally missing regions and dashed lines deleted regions.

However, contrary to capping, Ca^{2+} mobilization was entirely dependent on the presence of the EMPDs. In fact, deletion of this domain in both ε and γ isotypes (constructs ε-mSIP/ΔEMPD and γ1-mSIP/ΔEMPD) failed to induce Ca^{2+} mobilization following cross-linking (Fig. 3). This characteristic was also true for the ΔEMPD version of the complete IgE, indicating that it is an intrinsic property of the Ig and is not associated with the structure of the minireceptors. These results indicated that the presence of EMPD was essential for calcium signaling, even though the BCRs were still able to show membrane mobility leading to receptor capping.

ε-EMPD controls apoptotic signaling

Engagement of ε-ΔEMPD immunoreceptor constructs with anti-idiotypic Abs induced, in relatively short periods of time (6 h), the classical shrinkage observed in apoptotic cell death (data not shown). Analysis by the annexin V/PI assay revealed that a large proportion of cells (~80%) expressing ε-ΔEMPD receptors underwent apoptosis (Fig. 4*A*). This characteristic appeared to be specific for ε isotype, because engagement of γ1-ΔEMPD was not apoptotic (Fig. 4*B*). Furthermore, grafting of the γ1-EMPD into ε-mSIP/ΔEMPD restored the nonapoptotic activity of the receptor as well as the capacity to induce Ca^{2+} mobilization (Fig. 4*C*). Interestingly, although cross-linking of the ε_L immunoreceptors in both mSIP and mIgE was not apoptotic, the ε_{Sh} variant (also in mSIP and mIgE) was consistently moderately apoptotic (~15–20%) (Fig. 4*B*).

These results indicated that ε-EMPDs play a key role in controlling the capacity of membrane-bound IgE to induce apoptosis in the context of a mature isotype-switched B cell. The phenotype described for each immunoreceptor was independent of the level of expression, because in all cases several clones showing different levels of expression behaved in the same manner (data not shown).

As the anti-Id Abs were obtained from mice or guinea pigs (immunized with appropriate DNA constructs), they could bind to the low-affinity FcγR, FcγRIIB1 (CD32), expressed by A20 cells. The possibility that such receptor was involved in the apoptotic activity was ruled out by different experiments: first, the rat mAb anti-CD16/CD32 clone 2.4G2, which blocks binding to FcγRII and FcγRIII (23), was unable to reduce the apoptotic activity of either mouse or guinea pig anti-Id sera (data not shown); second, transfectomas derived from the FcγR negative A20 variant (A20IIA1.6) expressing ΔEMPD immunoreceptors showed the same behavior as the wt A20 cells (data not shown); third, Fab derived form anti-Id guinea pig sera showed to be functional in inducing apoptosis only when cross-linked with a secondary goat anti-guinea pig serum, unable to bind the murine FcγR (Fig. 4*D*). This result in addition demonstrates that binding of the Fab to the Id of the immunoreceptors was not sufficient to deliver the apoptotic signaling and that cross-linking was instead required.

Downloaded from http://www.jimmunol.org/ by guest on September 26, 2017

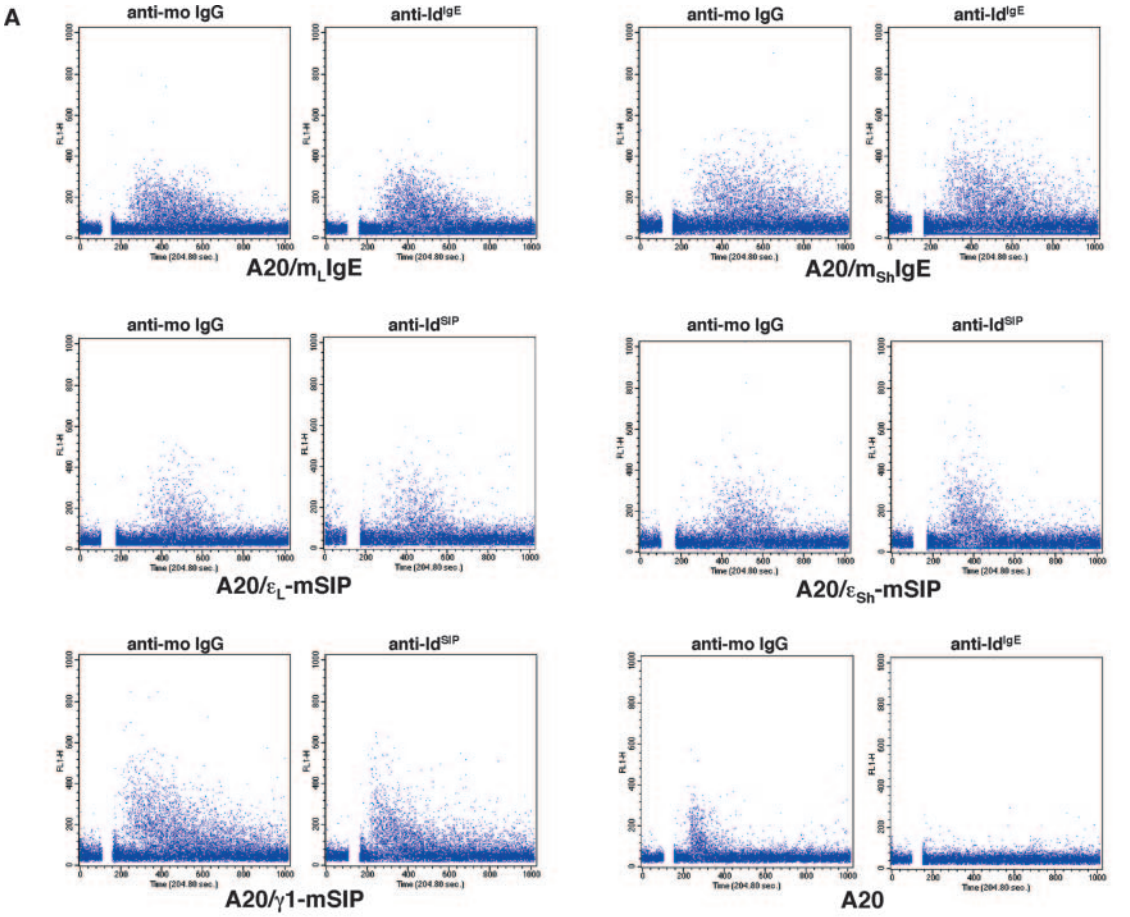

Downloaded from http://www.jimmunol.org/ by guest on September 26, 2017

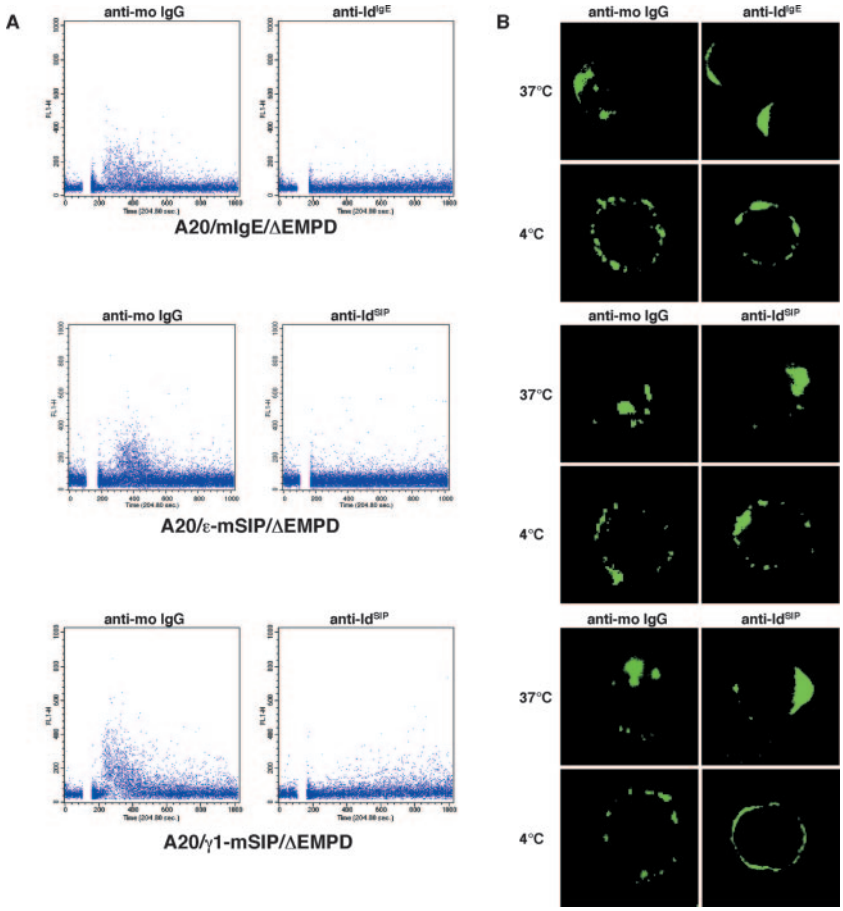

FIGURE 3. Calcium mobilization (*A*) and receptor aggregation (*B*) of Id-cross-linked ε (mIgE/ΔEMPD and ε-mSIP/ΔEMPD) and γ1 (γ1-mSIP/ΔEMPD) immunoreceptors with deleted EMPDs.

Activation of ERK

Because activation of MAPK ERK has been described to be involved in apoptotic signaling in immature B lymphocytes originating from the BCR (24, 25), we looked into the ability of the ε-ΔEMPD receptors to deliver a signal transduction leading to ERK phosphorylation following engagement. In the two cell lines expressing the mIgE/ΔEMPD and the ε-mSIP/ΔEMPD, we analyzed the pattern of ERK1/2 phosphorylation induced following cross-linking of the endogenous murine IgG as well as of the transfected ε receptor. As shown in Fig. 5*A*, the two ε-BCRs/ΔEMPD were able to induce ERK1/2 phosphorylation. However, in contrast to the endogenous murine IgG, which showed a peak of activity at ~10 min and then decreased, both ε receptors showed a significant longer period (up to 60 min) of ERK1/2 activation.

Apoptotic signaling through IgM BCR in the immature WEHI-231 B cell line was reported to be inhibited by simultaneous engagement of CD40 (26). As shown in Fig. 5*B*, partial rescue of apoptosis was also observed upon simultaneous cross-linking of the ε-ΔEMPD immunoreceptors and CD40. Interestingly, this activity was reflected as well in the modification of the kinetics of ERK phosphorylation, thus suggesting involvement of MAPKs.

Role of εCH4 domain

Because deletion of EMPD was sufficient to turn the ε-BCR into an apoptotic molecule, we decided to investigate the roles of the other domains to determine whether deletion of either of them alone, or in the ΔEMPD receptor, had any effect upon cross-linking. We started deleting either the εCH4 ectodomain, or the cytoplasmic tail (CytoD) alone, and found that none of them had any apoptotic effect (Fig. 6*A*). However, a double deletion mutant lacking both the EMPD and the CytoD (ε-mSIP/ΔEMPD/ΔCyto) was membrane expressed and fully competent in inducing apoptotis (>80%), indicating that signaling in the absence of EMPD was completely independent from the CytoD (Fig. 6*A*). To address whether the TMD was involved, the γ1 TMD and CytoD were grafted into the ε-ΔEMPD (ε-mSIP/ΔEMPD/γ1-TMD-Cyto). Upon cross-linking, this membrane-expressed chimera induced apoptosis, indicating that the distinct signaling of ε receptors does not reside in the ε-TMD nor in the cytoplasmic tail, but rather in εCH4 (Fig. 6*A*). This conclusion was further supported by the lack of apoptotic activity of an additional construct: a γ1-ΔEMPD chimera containing a γ1CH3 ectodomain with the TM-CytoD from ε isotype (construct γ1-mSIP/ΔEMPD/ε-TMD-Cyto) (Fig. 6*A*).

We obtained additional evidence of the involvement of εCH4 in the apoptotic signaling. We reasoned that if εCH4 were able to interact with an as yet undefined membrane component, it should be possible to induce apoptosis on wt A20 cells by exposing them to a secretory version of ε-SIP (i.e., devoid of EMPD, TMD, and CytoD), followed by cross-linking. As shown in Fig. 6*B*, when A20 cells were simultaneously incubated with a soluble ε-SIP and

FIGURE 2. Intracellular calcium mobilization (*A*) and immunofluorescence of BCRs (*B*) on the indicated cell lines, upon cross-linking of the endogenous mouse mIgG (anti-mo IgG), the Id expressed by the full-length human mIgE (anti-Id^{IgE}) or the Id of the SIP constructs (anti-Id^{SIP}). *A*, Cells labeled with Fluo-3AM were analyzed by real-time cytofluorimetry. *B*, Receptor aggregation (patching and capping) was induced incubating, respectively, at 4°C or 37°C, with the indicated cross-linkers.

Downloaded from http://www.jimmunol.org/ by guest on September 26, 2017

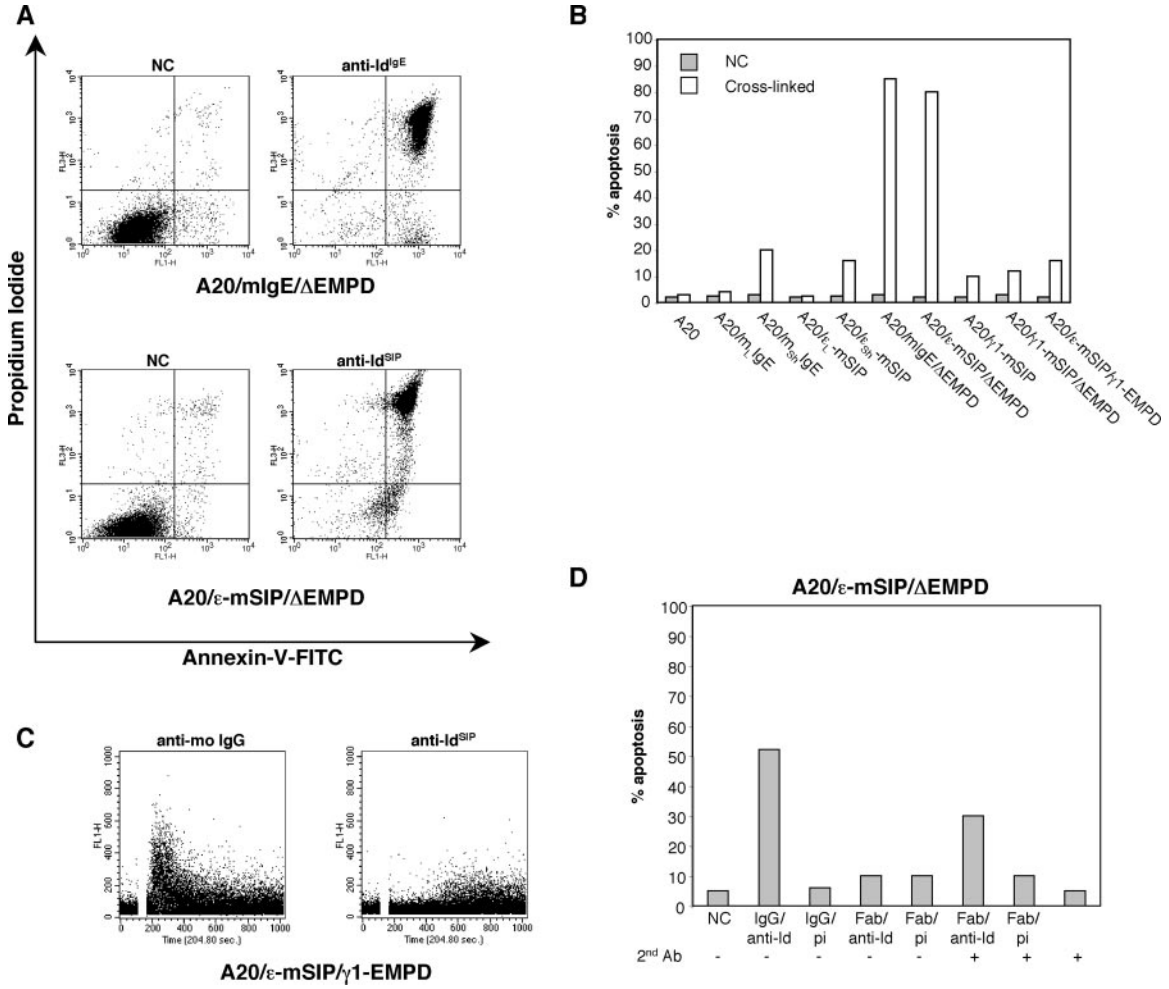

FIGURE 4. Apoptosis induction in EMPD-deleted ε immunoreceptors. *A*, Cytofluorimetry of annexin V/PI double staining of cells expressing mIgE or ε-mSIP lacking the EMPD, 15 h after cross-linking with specific anti-Id^{SIP} Abs. *B*, Comparison of anti-Id-induced apoptosis for the different immunoreceptors. *C*, Calcium mobilization in cells expressing the chimeric ε-mSIP containing the EMPD from γ1 isotype (construct ε-mSIP/γ1-EMPD). *D*, Apoptosis on cells expressing ε-mSIP/ΔEMPD, induced with Fab derived from anti-Id serum. Experiments were performed with equivalent amounts of purified anti-Id^{SIP} IgG (IgG/anti-Id) and Fab derived from the same preparation (Fab/anti-Id) or IgG and Fab derived from preimmune serum (IgG/preimmune and Fab/postinfection, respectively). When indicated, a secondary Ab (goat anti-guinea pig IgG, 2nd Ab), was added as a cross-linker.

an anti-Id serum, a significant number of cells underwent apoptosis. As expected, apoptosis required a specific anti-Id serum, because a control one did not have any effect.

Taken together, these results indicated that the εCH4 domain, displayed on the cell surface in the absence of tethering through the EMPD, is responsible for the apoptotic signaling, which appears to involve ERK phosphorylation, but not Ca^{2+} mobilization.

ΔEMPD immunoreceptor-mediated apoptosis does not involve activation of caspases

To explore the dependency on caspase activation of the apoptotic pathway of the ε-ΔEMPD immunoreceptors, we tested the effect of the broad range caspase inhibitor z-VAD-fmk. As shown in Fig. 7*A*, z-VAD-fmk did not inhibit cell death induced by anti-Id Abs. In contrast, cross-linking of the apoptotic caspase-dependent Fas receptor was completely abolished, indicating that apoptosis induced through the ε-ΔEMPD immunoreceptors was caspase independent. This conclusion was further confirmed by Western blot analysis of the caspase-3 substrate PARP. Contrary to Fas, ε-ΔEMPD cross-linking did not induce cleavage of PARP, as revealed by the persistence of the 116-kDa band of the uncleaved product (Fig. 7*B*), despite the reduction in the mitochondrial membrane potential (27), as revealed by cytofluorimetric analysis of cells labeled with the Mitotracker reagent (Fig. 7*C*). However, a significant increase in a cell population with a reduced DNA content was observed (Fig. 7*D*), although the characteristic pattern of DNA fragmentation into a nucleosome ladder (as shown by anti-Fas) was less apparent (Fig. 7*E*), probably reflecting the lack of caspase activation.

Discussion

B lymphocytes respond to Ags through engagement of the BCR by direct binding to the mIg. As a consequence, depending on the differentiation status of the B cells, the strength and duration of the interaction, presence or absence of costimulatory or inhibitory signals, cells are induced to proliferate and differentiate into plasma cells, or anergy or apoptosis is induced (28). In particular, mature B cells and memory B cells switched to IgA, IgG or IgE isotypes are recruited into germinal centers, where active somatic hypermutation leading to affinity maturation takes place. In this process, a large number of cells also fail to successfully engage Ag and die by apoptosis (15). The mechanism by which the BCR delivers apoptotic signaling is far from being clear (29, 30). Different regulation of BCR signaling through the B cell coreceptor CD22 was

Downloaded from http://www.jimmunol.org/ by guest on September 26, 2017

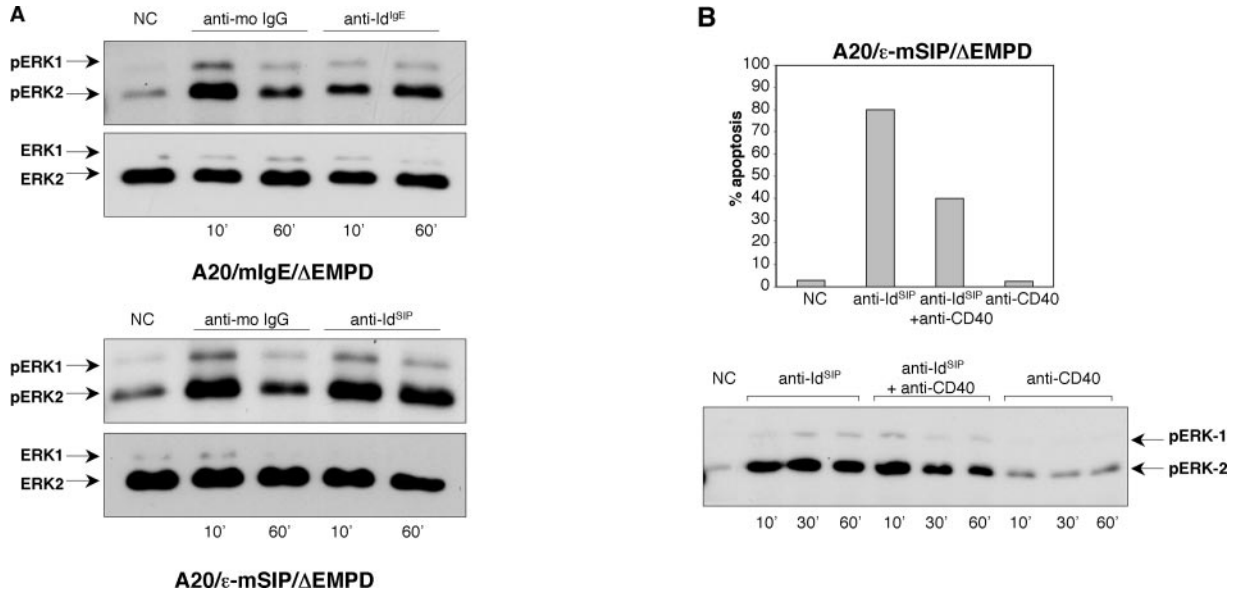

FIGURE 5. Activation of ERK1/2 MAPKs. *A*, Western blots of A20 cells expressing the two different ΔEMPD ε immunoreceptors (mIgE/ΔEMPD and ε-mSIP/ΔEMPD) following receptor engagement for the indicated time periods. Blots were developed with an anti-phospho-ERK1/2 mAb for activated ERK (*upper panels*), or with an anti-ERK1/2 for the total protein (*lower panels*). NC, Noncross-linked. *B*, Apoptosis and kinetics of ERK1/2 phosphorylation, upon coengagement of ε-mSIP/ΔEMPD and CD40. NC, Noncross-linked.

reported to be dependent on the distinct cytoplasmic tails (μ and γ) of the mIg isotypes (31). Also, for the ε-isotype, signal transduction was proposed to be different from other isotypes, including interactions of the cytoplasmic tail with specific cellular proteins (6, 32). Moreover, it was recently reported that IgE$^+$ cells could directly interact and trigger degranulation, in an Ag-independent manner, with mast cell and basophils expressing the FcεRI (33).

Diversity in the constitution of the different isotypes may conceal differences in their activities. Our observation that the EMPD plays a clearly distinct role in controlling apoptosis in mIgE and mIgG points in this direction. For the α, δ, and μ isotypes, the ΔEMPD versions were not well expressed, and therefore, no information could be obtained. In addition, among all isotypes, mIgE has the longest EMPD (in the most abundant ε_L version), with 66 aa and two of four cysteines involved in interchain disulfide bridges (9). The short version, however, presents a significantly higher apoptotic activity, although reduced when compared with the ΔEMPD. Because membrane short IgE has been shown to be apoptotic in immature B cells, this suggests that the cellular outcome depends on both the isoform expressed and the cellular context. Our findings that even in the mature A20 the mIgE can be apoptotic highlights the importance of the EMPD in controlling cell signaling.

Indeed, the Ca^{2+} mobilization experiments confirmed that signaling through the ΔEMPD receptors was essentially different, failing to activate Ca^{2+} release. Despite this, ERK1/2 phosphorylation, which has been implicated in BCR activation (34, 35) as well as in BCR-mediated apoptosis (25, 26), was nevertheless activated in the ΔEMPD receptors, although with a different kinetics. Consistent with these characteristics was the observation that costimulation of ε-ΔEMPD BCR and CD40 produced partial rescue of the apoptotic signaling and partial change of ERK phosphorylation kinetics.

It was reported recently that ERK acts as a kinase for the death-associated protein kinase, which in turn promotes ERK cytoplasmic retention, impairing ERK survival signals. Interestingly, the formation of ERK-death-associated protein kinase complex has been shown to be essential for promoting caspase-independent apoptosis in human D2 erythroblastic cells (36).

Despite several reports documenting activation via mitochondria of caspases 3 and 9 in BCR-mediated death signaling in both normal and B cell lymphomas (37–39), the apoptosis induced

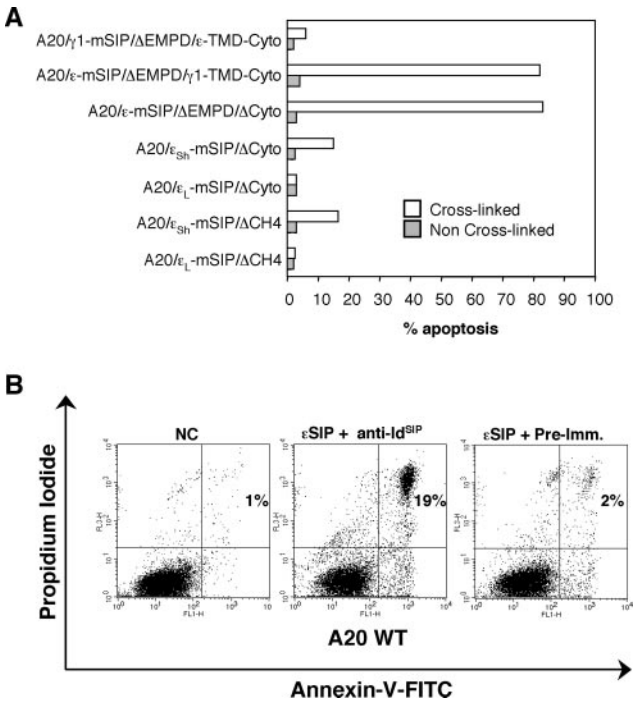

FIGURE 6. *A*, Apoptosis levels induced by anti-Id cross-linking of different mutant constructs of ε-mSIPs and γ1-mSIPs, determined by the annexin V/PI assay. *B*, Annexin V/PI assay of wt A20 cells nontreated (*left panel*) or treated with the secretory form of the ε-SIP, and cross-linked with the anti-Id^{SIP} serum (*central panel*) or the preimmune serum (*right panel*).

Downloaded from http://www.jimmunol.org/ by guest on September 26, 2017

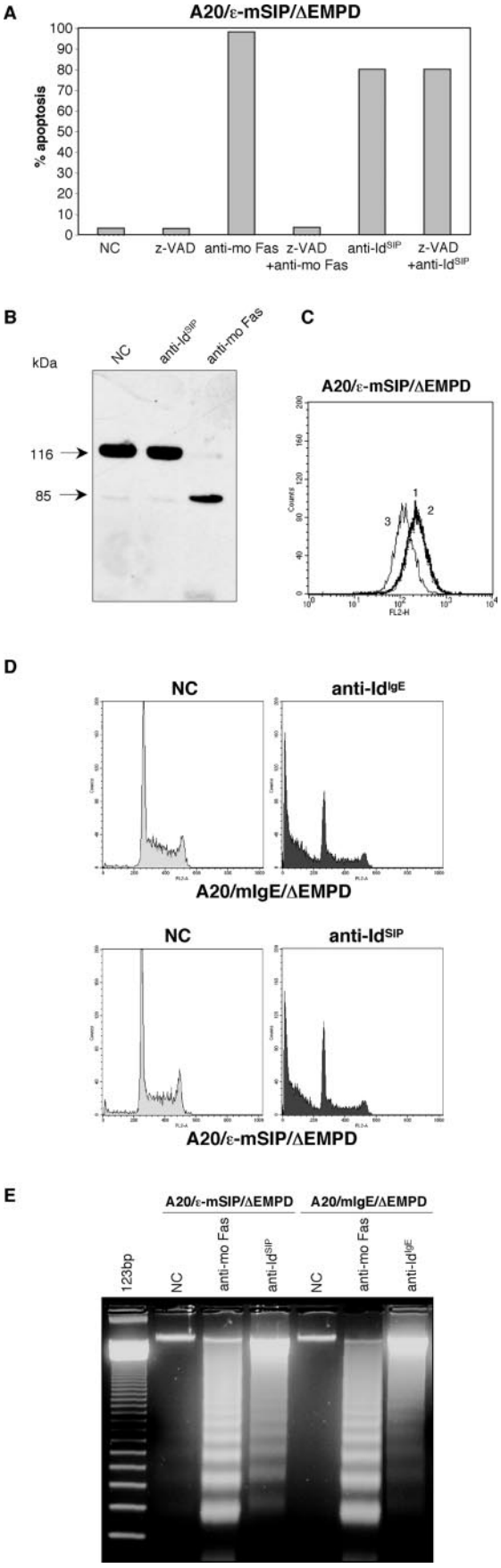

FIGURE 7. Lack of caspase activation in the apoptosis induced in A20 cells expressing ε-ΔEMPD immunoreceptors, upon BCR engagement. *A*, Apoptosis levels in the presence or absence of the caspase inhibitor z-VAD-fmk, determined by the annexin V/PI assay. Anti-Fas was used as a caspase-dependent apoptosis-positive control. *B*, Western blot analysis of PARP cleavage. Arrows indicate the position of full-length (116-kDa) and cleaved (85-kDa) PARP. *C*, Mitochondrial membrane potential determined in cells noncross-linked (1) or cross-linked with anti-mo IgG (2) and anti-Id^{SIP} (3). *D*, Cytofluorimetric analysis of cellular DNA content. *E*, DNA degradation into oligonucleosome fragments. NC, Noncross-linked.

through the ΔEMPD immunoreceptors was not dependent on caspase activation. Similar cases have been described previously also in mature T lymphocytes upon engagement of CD99 and in human monocytes and dendritic cells by anti-CD47 treatment (40, 41). Moreover, in the immature B cell line WEHI-231, signaling through IgM induced growth arrest and apoptosis in a caspase-independent mode that could be prevented by rescue signals mediated by CD40 (26, 27, 42). In this cell line, although IgM cross-linking induced caspase and cathepsin activities, these proteases were not responsible for BCR-mediated apoptosis, suggesting the existence of an alternative proteolytic pathway (43). Moreover, B cell responses appear to be normal in caspase-deficient mice, indicating that several apoptotic pathways coexist in mammalian cells, and suggesting that a single stimulus can induce the activation of more than one pathway (44). Our results showed that caspase independence was also characteristic of the apoptosis induced through the ΔEMPD ε-immunoreceptors in the mature B cell line A20. It is unlikely that other lysosomal cystein proteases, like cathepsins and calpains, were involved, because the inhibitor of these proteases, Loxistatin, was unable to block apoptosis (data not shown).

It has become clear that mitochondria play a key role in the control of cell fate, modulating cell survival and cell death. During apoptosis, mitochondrial alterations, such as loss of the mitochondrial $\Delta\psi$m, release of apoptogenic proteins (cytochrome *c*, apoptosis-inducing factor, endonuclease G), and decrease of ATP synthesis, occur (45). Cell death signaling through BCR causes dysfunction of mitochondria (46). We found that apoptosis induced by Id cross-linking induced mitochondrial damage, leading to a decrease of the $\Delta\psi$m. Because apoptosis was not mediated by caspases, it is possible that some other mitochondrial proteins such as apoptosis-inducing factor and endonuclease G may be responsible for the observed chromatin condensation and DNA cleavage (47).

In doing the cross-linking experiments, we observed that anti-idiotypic Abs were far more efficient than anti-Fc region Abs (data not shown). This result suggests that mIg signaling might involve additional structural constraints achieved by engagement through the V regions, as it is the case for Ag binding. In addition, when no apoptosis was detectable, we never observed proliferation upon cross-linking of the immunoreceptors.

We were able to map the εCH4 domain as the main responsible for the apoptotic signaling. The ability of a soluble SIP version to deliver apoptosis upon cross-linking strongly suggests that the interaction with a hitherto unidentified membrane component is at the base of the response. Furthermore, we have recently obtained additional evidence in this direction, showing that a GPI-anchored membrane version of the ε-mSIP/ΔEMPD was also apoptotic when transfected into A20 cells (data not shown).

Apoptosis of mIgE$^+$ cells could be at the base of the extremely low number of such cells found, in agreement with the requirement of membrane expression for production of serum IgE (6). Although we are aware of the limitations imposed by our model, the results presented show that the εBCR deleted of its EMPD delivers a strong apoptotic signal within the context of a mature isotype-switched B cell. However, this is not the case for the other Ig

Downloaded from http://www.jimmunol.org/ by guest on September 26, 2017

isotypes analyzed. We speculate that in vivo, neutralization of the ε-EMPD by a yet unknown mechanism might be at the base of the process that ends triggering apoptosis upon ε-BCR engagement, thus explaining the low proportion of circulating IgE^+ B cells. In this respect, mapping the apoptotic activity to the εCH4 suggests that this domain promotes new interactions of the ε-BCR with other apoptotic membrane components. Current experiments are oriented to the molecular characterization of such components.

Acknowledgments

We are grateful to Federica Benvenuti for helpful suggestions and critical reading of the manuscript, and to Fulvia Vascotto (Institut Curie, Paris, France) for supplying us the A20IIA1.6 cell line.

Disclosures

The authors have no financial conflict of interest.

References

1. Schamel, W. W., and M. Reth. 2000. Monomeric and oligomeric complexes of the B cell antigen receptor. *Immunity* 13: 5–14.
2. Shaw, A. C., R. N. Mitchell, Y. K. Weaver, J. Campos-Torres, A. K. Abbas, and P. Leder. 1990. Mutations of immunoglobulin transmembrane and cytoplasmic domains: effects on intracellular signaling and antigen presentation. *Cell* 63: 381–392.
3. Grupp, S. A., K. Campbell, R. N. Mitchell, J. C. Cambier, and A. K. Abbas. 1993. Signaling-defective mutants of the B lymphocyte antigen receptor fail to associate with Ig-α and Ig-βγ. *J. Biol. Chem.* 268: 25776–25779.
4. Geisberger, R., R. Crameri, and G. Achatz. 2003. Models of signal transduction through the B-cell antigen receptor. *Immunology* 110: 401–410.
5. Wakabayashi, C., T. Adachi, J. Wienands, and T. Tsubata. 2002. A distinct signaling pathway used by the IgG-containing B cell antigen receptor. *Science* 298: 2392–2395.
6. Achatz, G., L. Nitschke, and M. C. Lamers. 1997. Effect of transmembrane and cytoplasmic domains of IgE on the IgE response. *Science* 276: 409–411.
7. Kaisho, T., F. Schwenk, and K. Rajewsky. 1997. The roles of γ1 heavy chain membrane expression and cytoplasmic tail in IgG1 responses. *Science* 276: 412–415.
8. Weiser, P., R. Muller, U. Braun, and M. Reth. 1997. Endosomal targeting by the cytoplasmic tail of membrane immunoglobulin. *Science* 276: 407–409.
9. Bestagno, M., L. Vangelista, P. A. Mandiola, S. Mukherjee, J. Sepulveda, and O. R. Burrone. 2001. Membrane immunoglobulins are stabilized by interchain disulfide bonds occurring within the extracellular membrane-proximal domain. *Biochemistry* 40: 10686–10692.
10. Batista, F. D., D. G. Efremov, T. Tkach, and O. R. Burrone. 1995. Characterization of the human immunoglobulin ε mRNAs and their polyadenylation sites. *Nucleic Acids Res.* 23: 4805–4811.
11. Batista, F. D., D. G. Efremov, and O. R. Burrone. 1995. Characterization and expression of alternatively spliced IgE heavy chain transcripts produced by peripheral blood lymphocytes. *J. Immunol.* 154: 209–218.
12. Batista, F. D., S. Anand, G. Presani, D. G. Efremov, and O. R. Burrone. 1996. The two membrane isoforms of human IgE assemble into functionally distinct B cell antigen receptors. *J. Exp. Med.* 184: 2197–2205.
13. Pogue, S. L., and C. C. Goodnow. 1994. Ig heavy chain extracellular spacer confers unique glycosylation of the Mb-1 component of the B cell antigen receptor complex. *J. Immunol.* 152: 3925–3934.
14. Tisch, R., C. M. Roifman, and N. Hozumi. 1988. Functional differences between immunoglobulins M and D expressed on the surface of an immature B-cell line. *Proc. Natl. Acad. Sci. USA* 85: 6914–6918.
15. Guzman-Rojas, L., J. C. Sims-Mourtada, R. Rangel, and H. Martinez-Valdez. 2002. Life and death within germinal centres: a double-edged sword. *Immunology* 107: 167–175.
16. Chang, T. W. 2000. The pharmacological basis of anti-IgE therapy. *Nat. Biotechnol.* 18: 157–162.
17. Coyne, K. E., A. Crisci, and D. M. Lublin. 1993. Construction of synthetic signals for glycosyl-phosphatidylinositol anchor attachment: analysis of amino acid sequence requirements for anchoring. *J. Biol. Chem.* 268: 6689–6693.
18. Benvenuti, F., O. R. Burrone, and D. G. Efremov. 2000. Anti-idiotypic DNA vaccines for lymphoma immunotherapy require the presence of both variable region genes for tumor protection. *Gene Ther.* 7: 605–611.
19. Borsi, L., E. Balza, M. Bestagno, P. Castellani, B. Carnemolla, A. Biro, A. Leprini, J. Sepulveda, O. Burrone, D. Neri, and L. Zardi. 2002. Selective targeting of tumoral vasculature: comparison of different formats of an antibody (L19) to the ED-B domain of fibronectin. *Int. J. Cancer* 102: 75–85.
20. Benvenuti, F., and O. R. Burrone. 2001. Anti-idiotypic antibodies induced by genetic immunization are directed exclusively against combined V_L/V_H determinants. *Gene Ther.* 8: 1555–1561.
21. Cesco-Gaspere, M., F. Benvenuti, and O. R. Burrone. 2005. BCL1 lymphoma protection induced by idiotype DNA vaccination is entirely dependent on anti-idiotypic antibodies. *Cancer Immunol. Immunother.* 54: 351–358.
22. Jones, B., J. P. Tite, and C. A. Janeway, Jr. 1986. Different phenotypic variants of the mouse B cell tumor A20/2J are selected by antigen- and mitogen-triggered cytotoxicity of L3T4-positive, I-A-restricted T cell clones. *J. Immunol.* 136: 348–356.
23. Vuica, M., S. Desiderio, and J. P. Schneck. 1997. Differential effects of B cell receptor and B cell receptor-FcγRIIB1 engagement on docking of Csk to GTPase-activating protein (GAP)-associated p62. *J. Exp. Med.* 186: 259–267.
24. Lee, J. R., and G. A. Koretzky. 1998. Extracellular signal-regulated kinase-2, but not c-Jun NH_2-terminal kinase, activation correlates with surface IgM-mediated apoptosis in the WEHI 231 B cell line. *J. Immunol.* 161: 1637–1644.
25. Sutherland, C. L., A. W. Heath, S. L. Pelech, P. R. Young, and M. R. Gold. 1996. Differential activation of the ERK, JNK, and p38 mitogen-activated protein kinases by CD40 and the B cell antigen receptor. *J. Immunol.* 157: 3381–3390.
26. Gauld, S. B., D. Blair, C. A. Moss, S. D. Reid, and M. M. Harnett. 2002. Differential roles for extracellularly regulated kinase-mitogen-activated protein kinase in B cell antigen receptor-induced apoptosis and CD40-mediated rescue of WEHI-231 immature B cells. *J. Immunol.* 168: 3855–3864.
27. Katz, E., M. R. Deehan, S. Seatter, C. Lord, R. D. Sturrock, and M. M. Harnett. 2001. B cell receptor-stimulated mitochondrial phospholipase A_2 activation and resultant disruption of mitochondrial membrane potential correlate with the induction of apoptosis in WEHI-231 B cells. *J. Immunol.* 166: 137–147.
28. Gold, M. R. 2002. To make antibodies or not: signaling by the B-cell antigen receptor. *Trends Pharmacol. Sci.* 23: 316–324.
29. Niiro, H., and E. A. Clark. 2002. Regulation of B-cell fate by antigen-receptor signals. *Nat. Rev. Immunol.* 2: 945–956.
30. Eldering, E., and R. A. VanLier. 2005. B-cell antigen receptor-induced apoptosis: looking for clues. *Immunol. Lett.* 96: 187–194.
31. Silver, K., and R. J. Cornall. 2003. Isotype control of B cell signaling. *Sci. STKE* 2003: pe21.
32. Geisberger, R., M. Prlic, G. Achatz-Straussberger, I. Oberndorfer, E. Luger, M. Lamers, R. Crameri, U. Appenzeller, J. Wienands, M. Breitenbach, et al. 2002. Phage display based cloning of proteins interacting with the cytoplasmic tail of membrane immunoglobulins. *Dev. Immunol.* 9: 127–134.
33. Vangelista, L., E. Soprana, M. Cesco-Gaspere, P. Mandiola, G. Di Lullo, R. N. Fucci, F. Codazzi, A. Palini, G. Paganelli, O. R. Burrone, and A. G. Siccardi. 2005. Membrane IgE binds and activates FcεRI in an antigen-independent manner. *J. Immunol.* 174: 5602–5611.
34. Koncz, G., C. Bodor, D. Kovesdi, R. Gati, and G. Sarmay. 2002. BCR mediated signal transduction in immature and mature B cells. *Immunol. Lett.* 82: 41–49.
35. Jacob, A., D. Cooney, M. Pradhan, and K. M. Coggeshall. 2002. Convergence of signaling pathways on the activation of ERK in B cells. *J. Biol. Chem.* 277: 23420–23426.
36. Chen, C. H., W. J. Wang, J. C. Kuo, H. C. Tsai, J. R. Lin, Z. F. Chang, and R. H. Chen. 2005. Bidirectional signals transduced by DAPK-ERK interaction promote the apoptotic effect of DAPK. *EMBO J.* 24: 294–304.
37. Lens, S. M., B. F. den Drijver, A. J. Potgens, K. Tesselaar, M. H. van Oers, and R. A. van Lier. 1998. Dissection of pathways leading to antigen receptor-induced and Fas/CD95-induced apoptosis in human B cells. *J. Immunol.* 160: 6083–6092.
38. Berard, M., P. Mondiere, M. Casamayor-Palleja, A. Hennino, C. Bella, and T. Defrance. 1999. Mitochondria connects the antigen receptor to effector caspases during B cell receptor-induced apoptosis in normal human B cells. *J. Immunol.* 163: 4655–4662.
39. Herold, M. J., A. W. Kuss, C. Kraus, and I. Berberich. 2002. Mitochondria-dependent caspase-9 activation is necessary for antigen receptor-mediated effector caspase activation and apoptosis in WEHI 231 lymphoma cells. *J. Immunol.* 168: 3902–3909.
40. Pettersen, R. D., G. Bernard, M. K. Olafsen, M. Pourtein, and S. O. Lie. 2001. CD99 signals caspase-independent T cell death. *J. Immunol.* 166: 4931–4942.
41. Johansson, U., K. Higginbottom, and M. Londei. 2004. CD47 ligation induces a rapid caspase-independent apoptosis-like cell death in human monocytes and dendritic cells. *Scand. J. Immunol.* 59: 40–49.
42. Katz, E., C. Lord, C. A. Ford, S. B. Gauld, N. A. Carter, and M. M. Harnett. 2004. $Bcl\text{-}x_L$ antagonism of BCR-coupled mitochondrial phospholipase A_2 signaling correlates with protection from apoptosis in WEHI-231 B cells. *Blood* 103: 168–176.
43. Mlinaric-Rascan, I., and B. Turk. 2003. B cell receptor-mediated nuclear fragmentation proceeds in WEHI 231 cells in the absence of detectable DEVDase and FRase activity. *FEBS Lett.* 553: 51–55.
44. Hakem, R., A. Hakem, G. S. Duncan, J. T. Henderson, M. Woo, M. S. Soengas, A. Elia, J. L. de la Pompa, D. Kagi, W. Khoo, et al. 1998. Differential requirement for caspase 9 in apoptotic pathways in vivo. *Cell* 94: 339–352.
45. Bras, M., B. Queenan, and S. A. Susin. 2005. Programmed cell death via mitochondria: different modes of dying. *Biochemistry* 70: 231–239.
46. Bouchon, A., P. H. Krammer, and H. Walczak. 2000. Critical role for mitochondria in B cell receptor-mediated apoptosis. *Eur. J. Immunol.* 30: 69–77.
47. Daugas, E., S. A. Susin, N. Zamzami, K. F. Ferri, T. Irinopoulou, N. Larochette, M. C. Prevost, B. Leber, D. Andrews, J. Penninger, and G. Kroemer. 2000. Mitochondrio-nuclear translocation of AIF in apoptosis and necrosis. *FASEB J.* 14: 729–739.

Downloaded from http://www.jimmunol.org/ by guest on September 26, 2017